



A LETTERS JOURNAL EXPLORING  
THE FRONTIERS OF PHYSICS

OFFPRINT

**Thermoelectricity of Wigner crystal in a  
periodic potential**

O. V. ZHIROV and D. L. SHEPELYANSKY

EPL, **103** (2013) 68008

Please visit the new website  
[www.epljournal.org](http://www.epljournal.org)



A LETTERS JOURNAL EXPLORING  
THE FRONTIERS OF PHYSICS

## AN INVITATION TO SUBMIT YOUR WORK

[www.epljournal.org](http://www.epljournal.org)

### **The Editorial Board invites you to submit your letters to EPL**

EPL is a leading international journal publishing original, high-quality Letters in all areas of physics, ranging from condensed matter topics and interdisciplinary research to astrophysics, geophysics, plasma and fusion sciences, including those with application potential.

The high profile of the journal combined with the excellent scientific quality of the articles continue to ensure EPL is an essential resource for its worldwide audience. EPL offers authors global visibility and a great opportunity to share their work with others across the whole of the physics community.

### **Run by active scientists, for scientists**

EPL is reviewed by scientists for scientists, to serve and support the international scientific community. The Editorial Board is a team of active research scientists with an expert understanding of the needs of both authors and researchers.



**IMPACT FACTOR**  
**2.753\***  
\* As ranked by ISI 2010

[www.epljournal.org](http://www.epljournal.org)

**IMPACT FACTOR**

**2.753\***

\* As listed in the ISI® 2010 Science Citation Index Journal Citation Reports

**OVER**

**500 000**

full text downloads in 2010

**30 DAYS**

average receipt to online publication in 2010

**16 961**

citations in 2010  
37% increase from 2007

*“We’ve had a very positive experience with EPL, and not only on this occasion. The fact that one can identify an appropriate editor, and the editor is an active scientist in the field, makes a huge difference.”*

**Dr. Ivar Martin**

Los Alamos National Laboratory,  
USA

**Six good reasons to publish with EPL**

We want to work with you to help gain recognition for your high-quality work through worldwide visibility and high citations.

- 1 Quality** – The 40+ Co-Editors, who are experts in their fields, oversee the entire peer-review process, from selection of the referees to making all final acceptance decisions
- 2 Impact Factor** – The 2010 Impact Factor is 2.753; your work will be in the right place to be cited by your peers
- 3 Speed of processing** – We aim to provide you with a quick and efficient service; the median time from acceptance to online publication is 30 days
- 4 High visibility** – All articles are free to read for 30 days from online publication date
- 5 International reach** – Over 2,000 institutions have access to EPL, enabling your work to be read by your peers in 100 countries
- 6 Open Access** – Articles are offered open access for a one-off author payment

Details on preparing, submitting and tracking the progress of your manuscript from submission to acceptance are available on the EPL submission website [www.epletters.net](http://www.epletters.net).

If you would like further information about our author service or EPL in general, please visit [www.epljournal.org](http://www.epljournal.org) or e-mail us at [info@epljournal.org](mailto:info@epljournal.org).

**EPL is published in partnership with:**



European Physical Society



Società Italiana di Fisica



EDP Sciences

**IOP Publishing**

IOP Publishing



A LETTERS JOURNAL  
EXPLORING THE FRONTIERS  
OF PHYSICS

**EPL Compilation Index**

[www.epljournal.org](http://www.epljournal.org)



Biaxial strain on lens-shaped quantum rings of different inner radii, adapted from **Zhang et al** 2008 *EPL* **83** 67004.



Artistic impression of electrostatic particle-particle interactions in dielectrophoresis, adapted from **N Aubry and P Singh** 2006 *EPL* **74** 623.



Artistic impression of velocity and normal stress profiles around a sphere that moves through a polymer solution, adapted from **R Tuinier, J K G Dhont and T-H Fan** 2006 *EPL* **75** 929.

Visit the EPL website to read the latest articles published in cutting-edge fields of research from across the whole of physics.

Each compilation is led by its own Co-Editor, who is a leading scientist in that field, and who is responsible for overseeing the review process, selecting referees and making publication decisions for every manuscript.

- Graphene
- Liquid Crystals
- High Transition Temperature Superconductors
- Quantum Information Processing & Communication
- Biological & Soft Matter Physics
- Atomic, Molecular & Optical Physics
- Bose-Einstein Condensates & Ultracold Gases
- Metamaterials, Nanostructures & Magnetic Materials
- Mathematical Methods
- Physics of Gases, Plasmas & Electric Fields
- High Energy Nuclear Physics

If you are working on research in any of these areas, the Co-Editors would be delighted to receive your submission. Articles should be submitted via the automated manuscript system at [www.epletters.net](http://www.epletters.net)

If you would like further information about our author service or EPL in general, please visit [www.epljournal.org](http://www.epljournal.org) or e-mail us at [info@epljournal.org](mailto:info@epljournal.org)



**IOP Publishing**

**Image:** Ornamental multiplication of space-time figures of temperature transformation rules (adapted from T. S. Bíró and P. Ván 2010 *EPL* **89** 30001; artistic impression by Frédérique Swist).

# Thermoelectricity of Wigner crystal in a periodic potential

O. V. ZHIROV<sup>1,2</sup> and D. L. SHEPELYANSKY<sup>3</sup>

<sup>1</sup> *Budker Institute of Nuclear Physics - 630090 Novosibirsk, Russia*

<sup>2</sup> *Novosibirsk State University - 630090 Novosibirsk, Russia*

<sup>3</sup> *Laboratoire de Physique Théorique du CNRS (IRSAMC), Université de Toulouse, UPS F-31062 Toulouse, France, EU*

received 13 August 2013; accepted in final form 24 September 2013

published online 17 October 2013

PACS 84.60.Rb – Thermoelectric, electrodynamic and other direct energy conversion

PACS 72.20.Pa – Thermoelectric and thermomagnetic effects

PACS 73.20.-r – Electron states at surfaces and interfaces

**Abstract** – We study numerically the thermoelectricity of the classical Wigner crystal placed in a periodic potential and being in contact with a thermal bath modeled by the Langevin dynamics. At low temperatures the system has sliding and pinned phases with the Aubry transition between them. We show that in the Aubry pinned phase the dimensionless Seebeck coefficient can reach very high values of several hundreds. At the same time the charge and thermal conductivity of the crystal drop significantly inside this phase. Still we find that the largest values of  $ZT$  factor are reached in the Aubry phase and for the studied parameter range we obtain  $ZT \leq 4.5$ . We argue that this system can provide an optimal regime for reaching high  $ZT$  factors and realistic modeling of thermoelectricity. Possible experimental realizations of this model are discussed.

Copyright © EPLA, 2013

**Introduction.** – Computer microelectronic elements go to nanoscale sizes and the control of electrical currents and related heat flows becomes a technological challenge (see, *e.g.*, [1,2]). By the thermoelectric effect a temperature difference  $\Delta T$  generates an electrical current that can be compensated by a voltage difference  $\Delta V$ . The ratio  $S = \Delta V / \Delta T$  is known as the Seebeck coefficient, or thermopower, which plays an important role in the thermoelectric material properties. The thermoelectric materials are ranked by a figure-of-merit factor  $ZT = S^2 \sigma T / \kappa$  [3], where  $\sigma$  is the electric conductivity,  $T$  is the material temperature and  $\kappa$  is the thermal conductivity. To be competitive with usual refrigerators one needs to find materials with  $ZT > 3$  [1]. Various experimental groups try to reach this high value by skillful methods trying to reduce the thermal conductivity  $\kappa$  of samples keeping high electron conductivity  $\sigma$  and high  $S$  (see, *e.g.*, [4–8]). At room temperature the maximal values  $ZT \approx 2.4$  have been reached in semiconductor superlattices [4] while for silicon nanowires a factor  $ZT \approx 1$  has been demonstrated [5,6]. This shows that the volume reduction allows to decrease the thermal conductivity of lattice phonons and to increase  $ZT$  values.

It is interesting to consider the situations when the contribution of lattice phonons is completely suppressed to see if in such a case one can obtain even larger  $ZT$  factors.

Such extreme regime can be realized with an electron gas, *e.g.* in two dimensions (2DEG), where at  $T \sim 1$  K a contribution of lattice phonons is completely suppressed. In such a regime recent experiments [9] reported giant Seebeck coefficients  $S \sim 30$  mV/K obtained in a high resistivity domain.

While it is challenging to eliminate the contribution of lattice phonons experimentally it is rather easy to realize such a situation in numerical simulations simply replacing a lattice of atoms by a fixed periodic potential. After that we are faced with the problem of the thermoelectricity of the Wigner crystal in a periodic potential. In this letter we study this problem in one dimension (1D), which can be viewed as a mathematical model of silicon nanowires. We note that the ground state and low-temperature properties of this system in classical and quantum regimes have been investigated in [10]. It has been shown that at a typical incommensurate electron density the Wigner crystal slides easily in a potential of weak amplitude while above a critical amplitude the electrons are pinned by a lattice. The results [10] show that the properties of the Wigner crystal are similar to those of the Frenkel-Kontorova model where the transition between sliding and pinned phases is known as the Aubry transition [11] (see a detailed description in [12]). The positions of electrons on a periodic lattice are locally

described by the Chirikov standard map [13,14]. Similar dynamical properties appear also for the Wigner crystal in wiggling snaked nanochannels [15].

The previous studies of the Wigner crystal in a periodic potential [10] have been concentrated on analysis of the ground-state properties at lower temperatures. Here we analyze the transport properties of the crystal at finite temperatures studying its electron and thermal conductivities. Our approach allows to obtain the Seebeck coefficient and the figure of merit  $ZT$  at different regimes and various parameters. We note that there has been a significant interest in the heat transport and thermal conductivity in nonlinear lattices [16,17] but till present there have been no studies on thermoelectricity of interacting electrons in periodic lattices. We present the investigations of this generic case in this letter.

**Model description.** – The Hamiltonian of the 1D Wigner crystal in a periodic potential reads

$$H = \sum_i \left( \frac{p_i^2}{2} + K \cos x_i + \frac{1}{2} \sum_{j \neq i} \frac{1}{|x_i - x_j|} \right), \quad (1)$$

where  $x_i, p_i$  are the coordinate and momentum of the electron  $i$ ,  $K$  is an amplitude of periodic potential or lattice. As in [10] we use units  $e = m = k_B = 1$ , where  $e$  and  $m$  are the electron charge and mass,  $k_B$  is the Boltzmann constant and the lattice period is  $2\pi$ . The rescaling back to physical units is given in [10]. It is interesting to note that at  $e = k_B = 1$  we have  $S$  as a dimensionless coefficient, *e.g.*  $S = 30$  mV/K from [9] corresponds to  $S = 2585$ . Generally, in an ergodic regime induced by a developed dynamical chaos or thermal bath, one expects to have  $S \sim 1$  since a variation of potential or temperature should produce approximately the same charge redistribution. Thus, in our opinion, large values of the dimensionless Seebeck coefficient  $S$  indicate a strongly nonergodic regime of system dynamics. We will see below confirmations of this statement.

We concentrate our studies on a case of typical irrational electron density  $n_e = \nu/2\pi$ , per lattice period, given by the golden rotation number  $\nu = \nu_g = 1.618\dots$ . As in [10] we use the Fibonacci rational approximates with  $N$  electrons ( $0 \leq i \leq N - 1$ ) on  $M$  lattice periods (*e.g.*, 34 and 21 or 55 and 34).

According to [10] the Aubry transition at density  $\nu_g$  takes place at  $K = K_c = 0.0462$  so that the Wigner crystal is in a sliding phase for  $K < K_c$  and it is pinned by the potential at  $K > K_c$ . In the latter case there are exponentially many static configurations being exponentially close in energy to the Aubry cantori ground state. The sliding phase corresponds to the continuous Kolmogorov-Arnold-Moser (KAM) curves with  $\nu_g$  rotation number.

To study the thermoelectric effect (1) we add interactions with a substrate, which plays a role of a thermal bath with a given temperature distribution  $T(x)$  along the  $x$ -axis of the electron chain. We also add a static electric field  $E_{dc}$ .

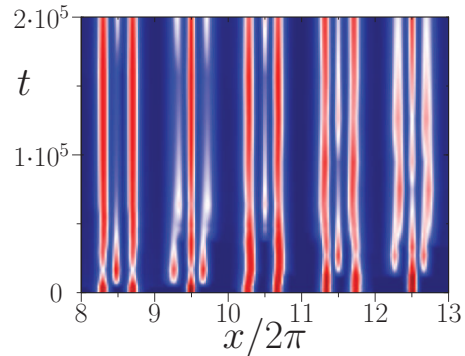


Fig. 1: (Colour on-line) Electron density variation in space and time from one Langevin trajectory at  $K/K_c = 2.6$ ,  $T/K_c = 0.11$ ,  $\eta = 0.02$ ,  $N = 34$ ,  $M = L/2\pi = 21$ ; density changes from zero (dark blue) to maximal density (dark red); only a fragment of  $x$  space is shown.

The thermal bath is modeled by the Langevin force (see, *e.g.*, [16]) so that the equations of electron motion are

$$\dot{p}_i = -\partial H/\partial x_i + E_{dc} - \eta p_i + g\xi_i(t), \quad \dot{x}_i = p_i. \quad (2)$$

Here, the parameter  $\eta$  phenomenologically describes dissipative relaxation processes, and the amplitude of Langevin force is given by the fluctuation-dissipation theorem  $g = \sqrt{2\eta T}$ . The normally distributed random variables  $\xi_i$  are as usually defined by correlators  $\langle \xi_i(t) \rangle = 0$ ,  $\langle \xi_i(t)\xi_j(t') \rangle = \delta_{ij}\delta(t - t')$ . The time evolution is obtained by the 4th-order Runge-Kutta integration with a time step  $\Delta t$ , at each such a step the Langevin contribution is taken into account. We checked that the results are not sensitive to the step  $\Delta t$  by its variation by a factor ten, the data are mainly obtained with  $\Delta t = 0.02$ . We use the hard-wall boundary conditions for electrons at the ends of the chain  $x = 0; L$  with the total system length  $L = 2\pi M$ . We also note that the Coulomb interaction couples all electrons in the sample. However, the results of [10,15] show that only nearest neighbors are effectively count. Due to that we present the numerical results for this approximation. We ensured that our results are not sensitive to including other neighbors.

A typical variation of the electron density in space  $x$  and time  $t$  is shown in fig. 1 for the Aubry pinned phase. Transitions, induced by thermal fluctuations, from one to two electrons inside one potential minimum are well visible.

**Numerical results for the Seebeck coefficient.** – To compute  $S$  we impose a constant temperature gradient on the Langevin substrate with a temperature difference  $\Delta T$  at the sample ends. Then we compute the local electron temperature  $T_e(x) = \langle p^2(x) \rangle_t$  where the time average of electron velocities are done over a large time interval with up to  $t = 10^7$ . To eliminate periodic oscillations along the chain we divide it on  $M$  bins of size  $2\pi$  and do all averaging inside each bin. Typical examples of variations of electron temperature  $T_e(x)$  and electron rescaled density  $\nu(x) = 2\pi n_e(x)$  along the chain are shown for a

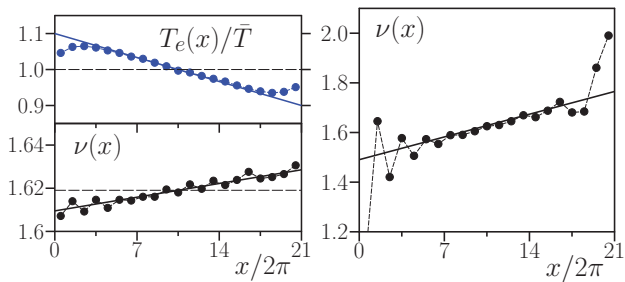


Fig. 2: (Colour on-line) Left panels: dependence of electron temperature  $T_e(x)$  (top, blue points) and rescaled density  $\nu(x)$  (bottom, black points) on the distance  $x$  along the chain placed on the Langevin substrate with a constant temperature gradient (blue line) at average temperature  $\bar{T} = 0.01$  and temperature difference  $\Delta T = 0.2\bar{T}$ ; the black line shows the fit of density variation in the bulk part of the sample. Right panel: density variation produced by a static electric field  $E_{dc} = 4 \times 10^{-4}$  at a constant substrate temperature  $T = 0.01$ ; the black line shows the fit of the gradient in the bulk part of the sample. Here  $N = 34, M = 21, K = 1.52K_c, \eta = 0.02$ , averaging is done over the time interval  $t = 10^7$ ;  $S = 3.3$  at  $T = 0.01 \approx 0.22K_c$ .

given  $\Delta T$  in fig. 2 (left panels). The chain ends are influenced by the boundary conditions, but in the main bulk part of the sample we obtain a linear gradient variation of  $T_e(x)$  and  $\nu(x)$ . The linear fit of  $T_e(x)$  and  $\nu(x)$  in the bulk part allows to determine the response of the Wigner crystal on the substrate temperature variation. In a similar way at fixed substrate temperature  $T$  we can find the density variation  $\nu(x)$  induced by a static field  $E_{dc}$  at the voltage difference  $\Delta V = E_{dc}L$ , as it is shown in fig. 2 (right panel). For the computation of  $S$  we find convenient to apply such a voltage  $\Delta V$  which at fixed  $T$  creates the same density gradient as those induced by the temperature difference  $\Delta T$  at  $E_{dc} = 0$ . Then by definition  $S = \Delta V/\Delta T$ . The data are obtained in the linear response regime when  $\Delta T, E_{dc}$  are sufficiently small.

The dependences of the obtained Seebeck coefficient  $S$  on  $K$  and  $T$  are presented in fig. 3. The data show that at  $K < K_c$  we have  $S \sim 1$  practically for all temperatures. Here the Langevin thermostat efficiently produces an ergodic distribution over all configurations of electrons and we have  $S \sim 1$  in agreement with the above ergodic argument. For  $K > K_c$  we find a significant increase of  $S$  at low temperatures  $T < K_c$ . In this regime the crystal is pinned by the lattice and different configuration states are separated by potential barriers  $\Delta U \sim K - K_c$  so that the transitions between configurations are suppressed by the Boltzmann factor  $\exp(-\Delta U/T)$ . Thus here long times are needed to have a transition between configurations [10]. In such a regime large voltage  $\Delta V$  is required to produce the same density gradient as those given by a fixed  $\Delta T$ . This leads to large  $S$  values generated by big and rare thermal fluctuations.

To check the stability of obtained results in the nonergodic regime with large  $S$  we use three different numerical

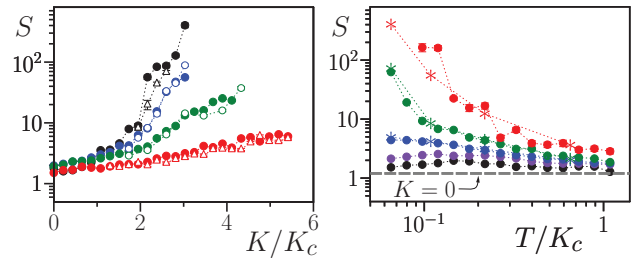


Fig. 3: (Colour on-line) Left panel: dependence of the Seebeck coefficient  $S$  on the rescaled potential amplitude  $K/K_c$  at temperatures  $T/K_c = 0.065, 0.11, 0.22$  and  $0.65$  shown by black, blue, green and red colours, respectively from top to bottom. The full and open symbols correspond, respectively, to chains with  $N = 34, M = 21$  and  $N = 55, M = 34$ . Right panel: dependence of  $S$  on  $T/K_c$  at different  $K/K_c = 0, 0.75, 1.5, 2.2, 3$  shown, respectively, by black, violet, blue, green and red points;  $N = 34, M = 21$ ; the dashed gray line shows the case  $K = 0$  for noninteracting particles. The stars show the corresponding results from the left plane at the same  $N, M$ . Dotted curves are drawn as a guide to the eye. Here and in other figures the statistical error bars are shown when they are larger than the symbol size. Here  $\eta = 0.02$ .

methods: a) *cold start* from the Aubry ground state at a given  $K$  and  $T = 0$ , followed by a warm up to the required  $T$  and then computing of the responses to a temperature gradient or electric field; in this approach the system evolves during a relaxation time  $t_{rel} \sim 10^6$  until the density response is stabilized, then the computations of gradients are performed on a time scale  $t_{com}$  determined by the condition of target statistical accuracy (typically  $t_{com} \sim 10^7$ ); b) *zero potential start* from the ground state at  $K = 0$  and given  $T$  followed by a sweep over  $K$  with a step  $\Delta K$  (typically  $\Delta K = 0.01$ ); at each step the responses of the current state to  $E_{dc}$  or  $\Delta T$  are determined; after  $t_{rel} = 5 \times 10^4$  the gradients are computed on times  $t_{com} \geq 10^4$  determined by target accuracy; the next step to  $K + \Delta K$  starts from the reached steady state at the previous  $K$  value, continuing up to the required  $K_{max}$  value, that completes one sweep in  $K$ ; then we repeat sweeps about 20 to 200 times to improve statistical accuracy; c) *hot start* from the Aubry ground state at given  $K$  with a warm up to  $T_{max} = 0.05 \approx K_c$ , followed by a sweep from  $T = T_{max}$  down to  $T = T_{min} = 0.003$  with equidistant steps in  $\ln T$ , in a way similar to b) with a similar number of sweeps.

The data in the left and right panels of fig. 3 are obtained by the methods b) and c), respectively. The stars in the right panel show the corresponding data from the left plane. A good agreement between methods b) and c) confirms the validity of the obtained results. The results from a more time-consuming method a) give a similar agreement with the methods b), c) of fig. 3 (data not shown). The comparison of results with  $N = 34$  and  $55$  electrons shows their independence of the chain length. However, at  $K \gg K_c$  and  $T \ll K_c$  very long computations are required to obtain statistically reliable results.

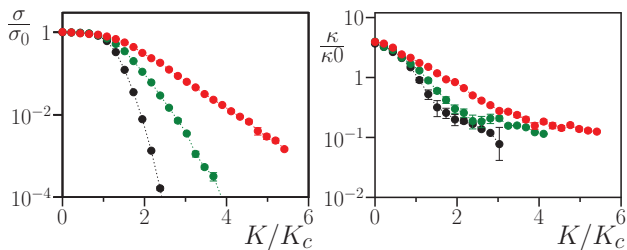


Fig. 4: (Colour on-line) Left panel: rescaled electron conductivity  $\sigma/\sigma_0$  as a function of  $K/K_c$  shown at rescaled temperatures  $T/K_c = 0.065, 0.22, 0.65$  by black, green and red points, respectively. Right panel: rescaled thermal conductivity  $\kappa/\kappa_0$  as a function of  $K/K_c$  shown at same temperatures and colours as in the left panel. Here we have  $N = 34, M = 21, \eta = 0.02, \sigma_0 = \nu_g/(2\pi\eta), \kappa_0 = \sigma_0 K_c$ .

The obtained results show that large values of  $S > 100$  can be reached in the pinned phase  $K > K_c$  at low temperatures. The growth of  $S$  is roughly proportional to the inverse Boltzmann factor. This nonergodic regime is characterized by big fluctuations. We think that a similar regime appeared in 2DEG experiments with even larger values  $S \sim 10^3$  [9].

#### Properties of charge and thermal conductivities.

– The large values of  $S$  do not guaranty high values of the figure-of-merit factor  $ZT$  which depends also on charge and thermal conductivities  $\sigma, \kappa$ .

To determine  $\sigma$  we use the periodic boundary conditions (electrons on a circle) and compute the average velocity  $v_{el}$  of the Wigner crystal in a weak electric field  $E_{dc}$  (acting along the circle) being in a linear response regime. The averaging is done over a typical time interval  $t = 10^7$  and over all electrons. Then the charge current is  $j = n_e v_{el} = \nu v_{el}/2\pi$  and  $\sigma = j/E_{dc}$ . In absence of potential at  $K = 0$  we have a crystal moving as a whole with  $v_{el} = E_{dc}/\eta$  and corresponding to the conductivity  $\sigma = \sigma_0 = \nu_g/(2\pi\eta)$  ( $\nu_g \approx 1.618\dots$ ). This theoretical result is well reproduced by numerical simulations as is shown in fig. 4 (left panel).

For  $K < K_c$  the conductivity  $\sigma$  is practically independent of  $T, K$ . However, for  $K > K_c$  we have a sharp exponential drop of  $\sigma$  with increasing  $K$  and decreasing temperature. This drop is satisfactorily described by the thermal activation dependence  $\sigma \propto \exp(-(K - K_c)/T)$ , at least when  $K$  is significantly larger  $K_c$ . We note that the temperature dependence differs significantly from those in 2DEG experiments [9] where resistivity becomes independent of  $T$  for  $T < 1$  K. We attribute this to 2D features of these experiments and to quantum effects being important at  $T \sim 1$  K. Indeed, the quantum fluctuations can produce sliding of the Wigner crystal even in the classically pinned phase as it is shown for 1D in [10].

Another important feature of  $\sigma$  variation with the system parameters is that  $\sigma \sim 1/\eta$  for  $K < K_c$  and that  $\sigma$  is practically independent of  $\eta$  for  $K > K_c$ . There is only

a moderate variation of  $S^2\sigma$  by a factor 4 when  $T/K_c$  changes from 0.1 to 10. We discuss this point in more detail later.

The thermal gradient produces not only the charge density variation but also a heat flow  $J$ . This flow is related to the temperature gradient by the Fourier law with the thermal conductivity  $\kappa$ :  $J = \kappa \partial T / \partial x$  (see, e.g., [2,16]). The flow  $J$  can be determined from the analysis of forces acting on a given electron  $i$  from left and right sides, respectively:  $f_i^L = \sum_{j < i} 1/|x_i - x_j|^2, f_i^R = -\sum_{j > i} 1/|x_i - x_j|^2$ . The time averaged energy flows, from left and right sides, to an electron  $i$  moving with a velocity  $v_i$  are, respectively,  $J_{L,R} = \langle f_i^{L,R} v_i \rangle_t$ . In a steady state the mean electron energy is independent of time and  $J_L + J_R = 0$ . But the difference of these flows gives the heat flow along the chain:  $J = (J_R - J_L)/2 = \langle (f_i^R - f_i^L) v_i / 2 \rangle_t$ . This computation of the heat flow, done with hard wall boundary conditions, allows us to determine the thermal conductivity via the relation  $\kappa = J L / \Delta T$ . Within numerical error bars we find  $\kappa$  to be independent of small  $\Delta T$  and number of electrons  $N$  ( $21 \leq N \leq 144$ ).

In principle, each electron interacts also with the substrate. However, in the central part of the chain the electron temperature is equal to the local temperature of the substrate due to local thermal equilibrium. This fact is directly seen in fig. 2 (left top panel, cf. blue points and straight line). Thus, we perform additional averaging of the heat flow in the central 1/3 part of the chain improving the statistical accuracy of data.

The dependence of the computed thermal conductivity  $\kappa$  on the amplitude of the potential  $K$  is shown in fig. 4 (right panel). It is convenient to present  $\kappa$  via a ratio to  $\kappa_0 = \sigma_0 K_c$  to have results in dimensionless units. Similar to the charge conductivity  $\sigma$ , we find that  $\kappa \approx 3.9\kappa_0$  at  $K < K_c$  being practically independent of temperature  $T$  for  $T < K_c$ . However, the transition to zero temperature and  $\eta = 0$  is singular due to divergence of  $\kappa$  in weakly nonlinear regular chains as discussed in [16].

In the pinned phase at  $K > K_c$  we see an exponential drop of  $\kappa$  with increase of  $K$  and decrease of  $T$  at  $T < K_c$ . As for  $\sigma$ , we find that for  $K > K_c$  the thermal conductivity is practically independent of dissipation rate  $\eta$ . We will discuss this in more detail below.

**Results for the figure-of-merit factor  $ZT$ .** – Now we determined all required characteristics and can analyze what  $ZT$  values are typical for our system and how  $ZT$  depends on the parameters.

The typical results are presented in fig. 5 where at the chosen parameters we have  $ZT < 3.5$ . At fixed  $T = 0.65K_c$  we have an optimal value of  $K$  with a maximum of  $ZT$  at a certain  $K \sim 2K_c$ , its position moves slightly to larger  $K$  with an increase of  $T$  (left panels). At fixed  $K = 2.6K_c$ , taken approximately at the maximum of  $ZT$  (left bottom panel), there is a visible logarithmic-type growth of  $ZT$  with increasing  $T$  approximately by a factor 7 in a range  $0.1 \leq T/K_c \leq 50$  (right panels). A further



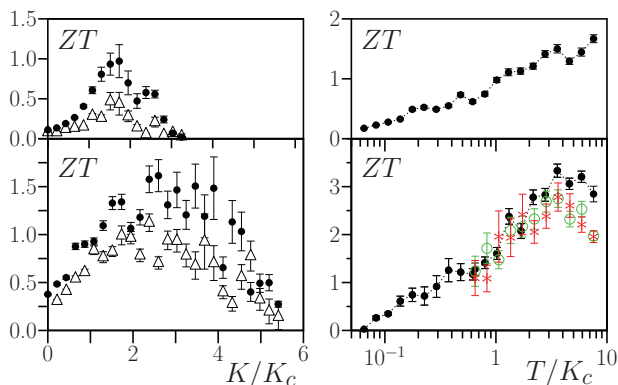


Fig. 5: (Colour on-line) Left panels: dependence of  $ZT$  on  $K/K_c$  at temperatures  $T/K_c = 0.11$  (top) and  $T/K_c = 0.65$  (bottom); the black points and open triangles correspond, respectively, to  $\eta = 0.02$  and  $\eta = 0.05$  at  $N = 34$ ,  $M = 21$ . Right panels: top, dependence of  $ZT$  on  $T/K_c$  for  $K/K_c = 0.75$  at  $\eta = 0.02$ ,  $N = 34$ ,  $M = 21$ ; bottom, the same as in the top panel at  $K/K_c = 2.6$  and  $N = 34$ ,  $M = 21$  (black points);  $N = 89$ ,  $M = 55$  (green circles);  $N = 144$ ,  $M = 89$  (red stars).

increase up to  $T \gg 5K_c \approx 0.25$  is not very interesting since then we start to have temperature to be larger than the energy of the Coulomb interaction  $E_W$  between electrons ( $T > E_W = \nu_g/2\pi \approx 0.25$ ) and the model goes to another limit of rigid-type balls which is not very realistic.

The results for two values of dissipation  $\eta = 0.02; 0.05$  shown in fig. 5 indicate that  $ZT$  drops with an increase of  $\eta$ . To understand the effects of  $\eta$  in a better way we show the dependence of the ratio  $R_S = S(\eta = 0.05)/S(\eta = 0.02)$  on  $K/K_c$  at fixed  $T/K_c = 0.65$  in fig. 6. The dependence of similar ratios  $R_\sigma$  and  $R_\kappa$  for  $\sigma$  and  $\kappa$  are also shown there. We find  $R_\sigma \approx R_\kappa \approx 0.5$  at  $K \ll K_c$  and  $R_\sigma \approx R_\kappa \approx 1$  for  $K > K_c$ . At  $K \ll K_c$  the ratios are close to the expected value 0.4 following from the theoretical scaling  $\sigma_0 \propto 1/\eta$  and from a similar expected dependence  $\kappa_0 \propto 1/\eta$ . However, in the pinned phase the dependence of  $\sigma$  and  $\kappa$  on  $\eta$  practically disappears. The physical mechanism of this effect is due to the fact that the electrons are pinned by the lattice and Wigner crystal phonons are localized, and hence, their mean free path becomes smaller than its value at  $K = 0$  when it is given by the dissipative exchange with the Langevin substrate. The ratio  $R_S$  is not sensitive to the variation of  $K/K_c$  even if  $S$  changes strongly with  $K$  (see fig. 3). A similar behaviour of ratios is obtained at lower  $T/K_c \approx 0.1$  with somewhat more sharp change between limit values 0.5 and 1 around  $K/K_c \approx 2$ . We also checked that the ratios constructed for other values of  $\eta$  (e.g.,  $\eta = 0.01, 0.1$ , instead of above  $\eta = 0.05$ ) also saturate at unit value for  $K/K_c > 2$ . Thus, at  $K/K_c > 2$ , the localization effects, induced by pinning, dominate over mean free path at  $K = 0$ .

The dependence of  $ZT$  on  $\eta$  is also shown in fig. 6. We see that a decrease of  $\eta$  generates a slow growth of  $ZT$  even if at so low value as  $\eta = 0.01$  we still have  $ZT < 2$ .

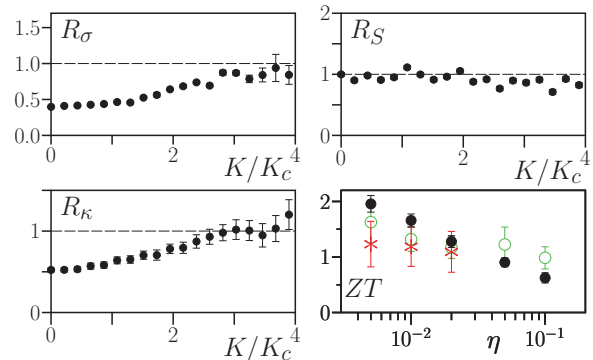


Fig. 6: (Colour on-line) Left panels: dependence of ratios  $R_\sigma$  (top) and  $R_\kappa$  (bottom) on  $K/K_c$  at  $T/K_c = 0.65$ . Right top panel: the same as in left panels for the ratio  $R_S$ . All ratios are defined in the text. Right bottom panel: dependence of  $ZT$  on  $\eta$  at  $T/K_c = 0.65$  at  $N = 34$ ,  $M = 21$  (black points);  $N = 89$ ,  $M = 55$  (green circles);  $N = 144$ ,  $M = 89$  (red stars) at fixed  $K/K_c = 2.6$  and  $T/K_c = 0.65$ .

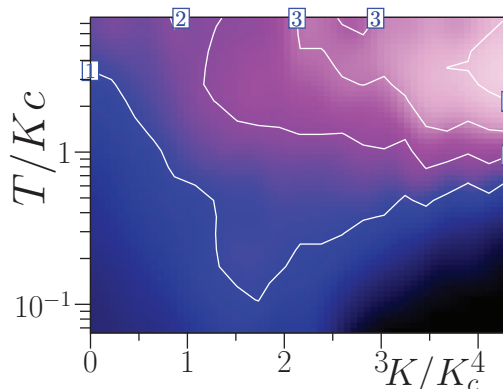


Fig. 7: (Colour on-line) Dependence of  $ZT$  on  $K/K_c$  and  $T/K_c$  shown by colour changing from  $ZT = 0$  (black) to maximal  $ZT = 4.5$  (light rose); contour curves show the values  $ZT = 1, 2, 3, 4$ . Here  $\eta = 0.02$ ,  $N = 34$ ,  $M = 21$ .

Here, we give numerical values of  $\eta$  in our computational units. It is more physical to look of a dimensionless ratio  $\eta/\omega_0$  where  $\omega_0$  is a maximal frequency of small oscillations near a vicinity of the Aubry ground state at  $K = K_c$ . According to the results [10] we have  $\omega_0 \approx 2\sqrt{K_c} \approx 0.4$ . Thus all our data are obtained in the regime of long relaxation time scale ( $\eta/\omega_0 \ll 1$ ). Also data obtained for longer chains  $N = 89$ ,  $M = 55$  and  $N = 144$ ,  $M = 89$  give no significant variation of  $ZT$  with chain length (see figs. 5,6).

The global dependence of  $ZT$  on  $K/K_c$  and  $T/K_c$  is presented in fig. 7 for the investigated parameter range  $T/K_c < 9$ ,  $K/K_c \leq 4.5$ . The maximal value  $ZT \approx 4.5$  is reached at the largest ratios  $K/K_c \approx 4.5$  and  $T/K_c \approx 4$ . However, at such large values of  $K, T$  we start to enter in the regime of potential and temperature being larger than the Coulomb energy  $E_W = \nu_g/2\pi$  so that it may be difficult to find materials which realize effectively such a

strong potential. For a more realistic condition  $T \leq K_c$  we have  $ZT < 2$ . We also note that for  $K > 5K_c \approx E_W$  the electrons are located in a strongly pinned phase with very strong fluctuations of transitions between different minima at  $T \leq K_c$ .

**Discussion.** – Our studies of the Wigner crystal in a periodic potential show that in the Aubry pinned phase at  $K > K_c$  the Wigner crystal has very larger Seebeck coefficients  $S$  which grow exponentially with a decrease of temperature or increase of the potential amplitude. However, at the same time the charge and thermal conductivities drop significantly. As a result, for all the variety of cases studied we obtain the maximal value of  $ZT \leq 2$  for the realistic parameter range  $K < 5K_c, T < K_c$ . Thus, there is a rather nontrivial compensation of three quantities  $S, \sigma, \kappa$  which determine the figure of merit,  $ZT$ . In total, the pinned phase has larger  $ZT$  values, compared to the sliding phase at  $K < K_c$ . For a high temperature  $T \approx 4K_c$  and strongly pinned regime  $K \approx 4K_c$  we even obtain  $ZT \approx 4$ . However, it remains questionable if such high potential amplitudes and temperatures are reachable in real materials.

We hope that it is possible to reach even larger  $ZT$  in the Aubry pinned phase at optimized system parameters. We find that  $ZT$  weakly increases with a decrease of the seed relaxation rate  $\eta$ . Thus a further decrease of  $\eta$  may allow to reach  $ZT > 3$  at low potential amplitudes  $K \approx 3K_c$  and temperatures  $T \approx K_c$ . However, special efforts should be performed to determine this seed  $\eta$  for real materials since in the pinned phase the charge and thermal conductivities drop significantly, compared to the sliding phase, becoming practically independent of seed relaxation rate.

It is also possible that further temperature increase significantly above  $T > 5K_c$  may produce even  $ZT > 5$  at  $K > 5K_c$ . However, the growth of  $ZT$  with  $T$  is slow, being close to a logarithmic growth, so that such high  $T$  and  $K$  may be not interesting in practice.

Thus the task to reach  $ZT > 3$  at low temperatures seems to be hard even in our simple model where the thermal conductivity of atomic lattice phonons is eliminated from the beginning and only electronic conductivity contribution is left. In this sense our model provides a superior bound for the  $ZT$  factor in 1D. We expect that for the Wigner crystal in two- and three-dimensional potentials the factor  $ZT$  will be reduced, compared to 1D case, since it will be more difficult to localize the phonons of a Wigner crystal. Thus, in a certain sense we expect that our model provides the most optimal conditions for large  $ZT$  values and still we remain at  $ZT < 2$  for realistic not very high temperatures  $T < K_c$ .

Finally, we provide some physical values of our model parameters. In physical units we can estimate the critical potential amplitude as  $U_c = K_c e^2 / (\epsilon d)$ , where  $\epsilon$  is a

dielectric constant,  $\Delta x$  is a lattice period and  $d = \nu \Delta x / 2\pi$  is a rescaled lattice constant [10]. For values typical for a charge density wave regime [18] we have  $\epsilon \sim 10, \nu \sim 1, \Delta x \sim 1 \text{ nm}$  and  $U_c \sim 40 \text{ mV} \sim 500 \text{ K}$  so that the Aubry pinned phase should be visible at room temperature. The obtained  $U_c$  value is rather high that justifies the fact that we investigated thermoelectricity in the frame of the classical mechanics of interacting electrons. In any case the real thermoelectric devices should work at room temperature and in this regime the classical treatment of electron transport can be considered as a good first approximation.

We think that it would be useful to perform experimental studies of electron transport in a periodic potential. We hope that such type of experiments can be possible with charge density waves (see, *e.g.*, [18] and references therein), strongly interacting electrons in ultraclean carbon nanotubes with interaction energies of 100 mV [19], experiments with electrons on a surface of liquid helium [20], and cold ions in optical lattices [21].

\*\*\*

The research of OVZ was partially supported by the Ministry of Education and Science of Russian Federation.

## REFERENCES

- [1] MAJUMDAR A., *Science*, **303** (2004) 777.
- [2] GOLDSMID H. J., *Introduction to Thermoelectricity* (Springer, Berlin) 2009.
- [3] IOFFE A. F., *Semiconductor Thermoelements, and Thermoelectric Cooling* (Infosearch, Ltd) 1957; IOFFE A. F. and SYIL'BANS L. S., *Rep. Prog. Phys.*, **22** (1959) 167.
- [4] VENKATASUBRAMANIAN R. *et al.*, *Nature*, **413** (2001) 597.
- [5] HOCHBAUM A. I. *et al.*, *Nature*, **451** (2008) 163.
- [6] BOUKAI A. I. *et al.*, *Nature*, **451** (2008) 168.
- [7] POUDEL B. *et al.*, *Science*, **320** (2008) 634.
- [8] BISWAS K. *et al.*, *Nature*, **489** (2012) 414.
- [9] NARAYAN V. *et al.*, *Phys. Rev. B*, **86** (2012) 125406.
- [10] GARCIA-MATA I., ZHIROV O. V. and SHEPELYANSKY D. L., *Eur. Phys. J. D*, **41** (2007) 325.
- [11] AUBRY S., *Physica D*, **7** (1983) 240.
- [12] BRAUN O. M. and KIVSHAR YU. S., *The Frenkel-Kontorova Model: Concepts, Methods, Applications* (Springer-Verlag, Berlin) 2004.
- [13] CHIRIKOV B. V., *Phys. Rep.*, **52** (1979) 263.
- [14] CHIRIKOV B. V. and SHEPELYANSKY D. L., *Scholarpedia*, **3** (2008) 3550.
- [15] ZHIROV O. V. and SHEPELYANSKY D. L., *Eur. Phys. J. B*, **82** (2011) 63.
- [16] LEPRI S., LIVI R. and POLITI A., *Phys. Rep.*, **377** (2003) 1.
- [17] LI N. *et al.*, *Rev. Mod. Phys.*, **84** (2012) 1045.
- [18] BRAZOVSKII S. *et al.*, *Phys. Rev. Lett.*, **108** (2012) 096801.
- [19] DESHPANDE V. V. *et al.*, *Science*, **323** (2009) 106.
- [20] REES D. G. *et al.*, *Phys. Rev. Lett.*, **106** (2011) 026803.
- [21] PRUTTIVARASIN T. *et al.*, *New J. Phys.*, **13** (2011) 075012.